

Cite this: *Lab Chip*, 2011, **11**, 1228

www.rsc.org/loc

PAPER

Non-emissive colour filters for fluorescence detection†‡

Mikihide Yamazaki,^a Oliver Hofmann,^b Gihan Ryu,^b Li Xiaoe,^a Tai Kyu Lee,^c Andrew J. deMello^{ab} and John C. deMello^{*ab}

Received 29th November 2010, Accepted 21st February 2011

DOI: 10.1039/c0lc00642d

We describe a simple technique for fabricating non-emissive colour filters based on the sensitisation of a highly porous nanostructured metal-oxide film with a monolayer of dye molecules. Ultrafast electron transfer at the oxide/dye interface induces efficient quenching of photogenerated excitons in the dye, reducing the photoluminescence quantum yield by many orders of magnitude. The resultant filters exhibit much less autofluorescence than conventional colour filters (where the chromophore is dispersed in a glass or polymer host), and are a viable low cost alternative to interference filters for microfluidic devices and other applications requiring non-emissive filtering.

Introduction

Microfluidic devices are attracting interest for point-of-care diagnostics due to their low unit cost, low usage of sample and reagents, fast analysis times, portability, and ability to manipulate small amounts of fluid.^{1,2} Typical stages in a diagnostic process include analyte sampling, sample pre-treatment, chemical reaction, analyte separation, and analyte detection. The last of these steps is often the most challenging due to the small quantities of analyte present and the consequent need for high sensitivity detection. In practice, optical methods – most notably fluorescence detection – are often the only ones that can provide adequate sensitivity. Considerable efforts have therefore been devoted to developing high performance optical components for use in microfluidic devices, including both active components such as light-sources^{2–6} and photodetectors^{2,4,5,7–10} and passive components such as prisms,⁸ microlenses,¹¹ filters,¹² mirrors,¹³ gratings,¹⁴ waveguides,^{15,16} and polarisers.¹⁷ Frequently, it is the performance of the passive components rather than the active ones that determines the final sensitivity of the system.^{12,18,19}

Optical long-pass filters play a particularly important role in microfluidic devices. In conventional fluorescence detection, the excitation source and detector are usually arranged orthogonally to one another to prevent direct illumination of the detector by the excitation source. This orthogonal geometry, however, is

difficult to implement in a microfluidic environment since it requires the production of optical-grade side-surfaces onto which optical components must somehow be mounted. The light source and detector are most conveniently placed on the upper and lower faces of the microfluidic chip in a face-on geometry. But this would ordinarily flood the detector with direct light from the excitation source, masking the typically weak fluorescence signal from the analyte. The key to discriminating the emission light from the excitation light in this face-on configuration is the use of a long-pass filter in front of the detector to block the excitation light and pass only the longer wavelength emission signal. The use of long-pass filters for this purpose is well established, but considerable difficulties are encountered when (as required for monolithic integration) the filter is placed in close proximity to the detector. In such circumstances any auto-fluorescence from the filter will add to the analyte-fluorescence, and so set a baseline beneath which it is difficult to measure a signal.

Autofluorescence is a particular problem for colour filters formed by dispersing pigments or dye molecules in a glass or polymer host.¹² For the detection of low analyte concentrations, even very weak auto-fluorescence from the filter may obscure the desired signal, so it is essential to select dyes that not only have acceptable blocking and transmission characteristics but ones that are also *completely* non-emissive. Needless to say the palette of usable materials is extremely limited. Auto-fluorescence can be largely avoided by switching to interference filters that comprise an alternating stack of high and low refractive index materials.^{20,21} Interference filters typically have excellent characteristics in terms of strong blocking in the stop-band, high transmission in the pass-band, sharp roll-on and extremely low auto-fluorescence, but they are expensive to produce due to the complex multistep nature of their fabrication and hence are ill-suited to low cost disposable applications. They also suffer from angular variability in their blocking/transmission characteristics, which can degrade their performance in actual use.²¹

^aDepartment of Chemistry, Imperial College London, South Kensington, London, United Kingdom SW7 2AZ. E-mail: j.demello@imperial.ac.uk

^bMolecular Vision Ltd, 90 Fetter Lane, London, United Kingdom EC4A 1J
^cNano-Pac Co. Ltd, Yeongtong-dong, Yeongtong-gu, Suwon-si, Gyeonggi-do, Korea

† Published as part of a LOC themed issue dedicated to UK Research: Guest Editors Professors Hywel Morgan and Andrew deMello.

‡ Electronic supplementary information (ESI) available: ESI Fig. 1–3. See DOI: 10.1039/c0lc00642d

Recently Richard and co-workers showed that, by combining interference filters with low-fluorescence colour filters, it is possible to produce high quality hybrid filters with very low auto-fluorescence and minimal angular variation.²¹ Any solution based on interference filters, however, is likely to be restricted to high-end applications where cost is of secondary concern. Indeed, without a departure from the traditional fabrication methods of sputtering, evaporation and chemical vapour deposition, it is doubtful whether interference filters could ever form a part of an ultra low cost disposable diagnostic technology.

In this paper we evaluate a purely dye-based approach to fabricating high performance optical filters that avoids the expense and angular variability of interference filters, whilst overcoming the undesirable auto-fluorescence characteristics of conventional colour filters. Our approach exploits ultrafast electron-transfer between a photo-excited dye molecule and a transparent metal oxide onto which the molecule is absorbed²²—the same process that forms the basis for the charge-generation step in dye-sensitised solar cells. In essence, a monolayer of the dye molecule is adsorbed onto the surface of a highly porous metal-oxide such as titania (TiO_2), generating a diffuse interface between the two materials. The interface acts as an extremely efficient quenching site for the photo-excited exciton,²³ reducing the photoluminescence quantum yield of the dye to a negligible level without appreciably perturbing its absorption characteristics. The oxide itself has a wide optical gap (*e.g.* $\Delta E > 3.2$ eV for titania), so does not absorb over the visible wavelength range typically used for diagnostic tests. Hence, providing the crystallite size is significantly smaller than the wavelength of light so as to minimise optical scattering, the oxide serves as an invisible scaffold for the dye molecule.

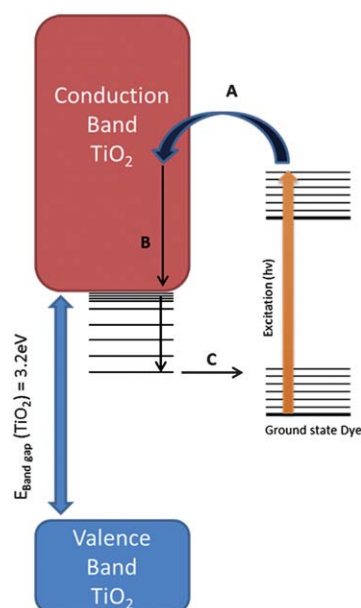


Fig. 1 Electron transfer process in dye-sensitised titania. (A) Ultrafast electron transfer from the anti-bonding orbitals of the dye to the conduction band of titania (TiO_2). (B) Thermalisation of the hot electron, followed by hopping between sub-gap titania sites. (C) Charge recombination with a proximate dye cation.

The mechanism of the quenching process is well established, see Fig. 1.²³ When an adsorbed dye molecule absorbs a photon, an electron is promoted to an unoccupied molecular orbital and from there undergoes ultrafast charge injection into the continuum of conduction band states in the titania. The electron relaxes by internal conversion to the conduction band-edge and then hops between titania sites until it reaches an interface with a dye-cation, whereupon it recombines non-radiatively to regenerate the dye. Importantly, the initial charge-transfer step from the dye to the oxide typically occurs on a very short time-scale ($\ll 100$ fs),^{23–27} meaning the photo-excited electron is removed from the dye molecule long before it has a chance to relax radiatively to the ground-state. In this way, it is possible to reduce the fluorescence quantum yield of the dye molecule to a negligible level and so quench the auto-fluorescence by many orders of magnitude.

Experimental

Titania films of approximate thickness $4.4\ \mu\text{m}$ were prepared by screen-printing an as-received commercial gel (WA-15DPT, Nanopac, South Korea) onto glass substrates and then curing in an oven at $450\ ^\circ\text{C}$ for 30 min, ramping the temperature gradually over a 15 min period to avoid cracking. A scanning electron micrograph of a typical titania film is shown in Fig. 2. The dominant grain size is < 50 nm, resulting in minimal optical scattering and an essentially invisible surface onto which dye molecules may be adsorbed. Each titania-coated substrate was then immersed overnight in a $0.01\ \text{M}$ solution of one of the following six dyes: Alizarin, Alizarin Red, Purpurin, Fluorescein, Fluorescein Disodium Salt (FDS) and Eosin Y—all of which were chosen for their ability to adsorb directly onto titania without surface functionalisation. The stained films were then washed repeatedly with acetone to remove unattached dye molecules and finally dried in a stream of nitrogen. Alizarin, Alizarin Red and Purpurin are anthraquinone-derived dyes with relatively low quantum efficiencies in solution in the range 0.2 to 3%,^{24,28} while the others are fluorescein derivatives with high efficiencies in the range 40 to 97%.²⁹ We note that dispersion in a polymer or glass host—the standard procedure for preparing colour filters—would in all cases be expected to yield substantially auto-fluorescent films.

For comparative purposes one of the dyes, FDS, was selected for dispersion in a polymer host to fabricate a conventional

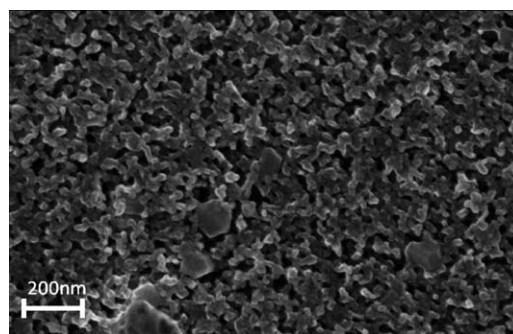


Fig. 2 Scanning electron micrograph of a nano-porous titania substrate, taken at $\times 200\ 000$ magnification and 1.5×10^{-9} atm.

colour filter. Adapting the method outlined in ref. 9, a 1 ml saturated solution of FDS was prepared in methanol and mixed with 20 g of poly(dimethylsiloxane) (PDMS) monomer and hardener pre-mixed at a ratio of 10 : 1 v/v (Sylgard 184 silicone elastomer kit, Dow Corning, Coventry, UK). The resulting solution was mixed vigorously until a uniform PDMS colouring was achieved. The dyed PDMS was then poured into a plastic mould and left to cure at room temperature for 48 h, resulting in a coloured film of approximate thickness 5 mm.

The transmission characteristics of the home-made filters and those of three commercially sourced Schott glass colour filters (GG475, OG530, OG550) were measured with a dual-beam UV/Vis spectrometer (Philips Unicam, UK), keeping the reference path empty so as to determine the overall transmission properties of the filters (dye plus substrate as opposed to the dye alone). Autofluorescence spectra were obtained by directing a 1.1 mW beam from a 442 nm HeCd laser (IK5552R-F, Kimmon Japan) onto the front side of each filter and placing a fibre-optic coupled to a CCD spectrometer (QE65000, Ocean Optics US) against the rear-side of the filter immediately behind the laser spot (see ESI Fig. 1†). This configuration broadly mimics the typical situation in a microfluidic device where the light-source and photodetector are directly opposite one another, and a long-pass filter is placed immediately in front of the photodetector to block the excitation light. Integration times of up to 15 min were used to collect the spectra due to the weak emission from the dye-sensitised titania films.

Results and discussion

Fig. 3(A) shows the absorption spectra of the six dye-sensitised titania films (note, additional information about the spatial uniformity of the filters is provided in ESI Fig. 3†). Although there are significant differences between the spectra, each one shows a rather broad cut-on from the short wavelength stop-band to the long wavelength pass-band with the absorbance approaching zero at ~800 nm. The absorbance in the stop-band was in all cases relatively small, falling as low as 1.7 for Purpurin, 1.5 for Alizarin, 1.2 for Alizarin Red, 0.5 for Fluorescein, 1.5 for FDS, and 0.4 for Eosin Y. Whilst these values are certainly too low for use as high performance long-pass filters, improved blocking can be achieved by stacking several dye-sensitised films on top of one another, although this is obviously at the expense of transmission in the pass-band. Fig. 3(B) shows the absorption spectrum for the FDS-doped PDMS film and the three Schott glass colour filters. The high baseline of the FDS-doped PDMS filter is due to the difficulty of achieving a uniform dispersion of FDS in PDMS at high concentration, which results in a cloudy highly scattering film. Also shown for comparison are the calculated absorption spectra for four-layer FDS- and Alizarin-sensitised titania stacks, obtained by multiplying the single-layer spectrum by four. (Note, direct measurement of the stack absorbance was not possible due to signal saturation in the vicinity of the absorption peaks at ~500 nm).

Fig. 4(A) shows the emission characteristics of the three Schott glass colour filters, the FDS-doped PDMS film and the four-layer FDS-sensitised titania stack, measured in the manner described above. It is evident that the three Schott glass filters and the dye-doped PDMS filter exhibit strong auto-fluorescence

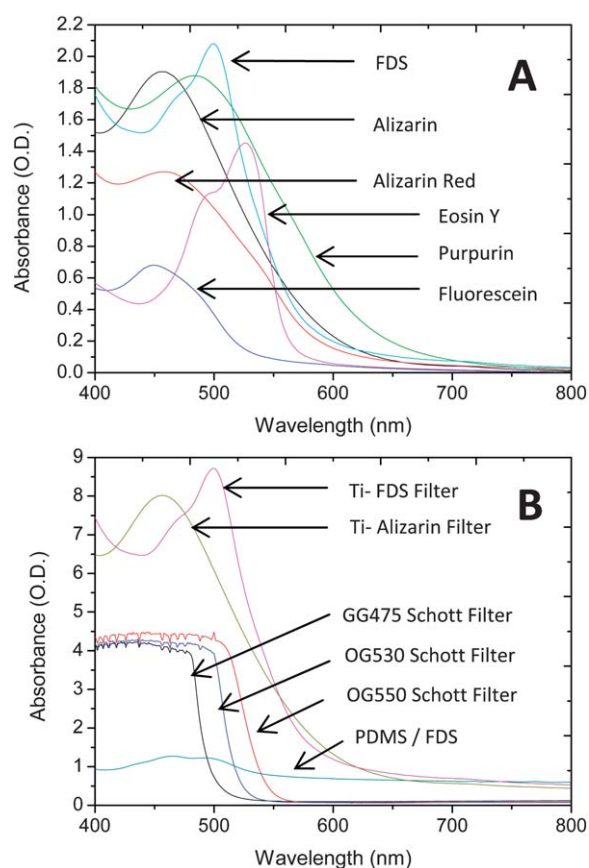


Fig. 3 (A) Absorption spectra of single-layer titania films sensitised with various anthraquinone- and fluorescein-derived dyes. (B) Absorption spectra of three commercially sourced Schott glass colour filters, and an FDS-doped PDMS filter; also shown for comparison are calculated absorption spectra for four-layer FDS- and Alizarin-sensitised titania stacks determined from the single-layer absorption spectra in 3(A).

that would preclude their use in high sensitivity detection. The FDS-sensitised titania film, however, exhibited extremely weak fluorescence that we were unable to detect even with a fifteen minute integration time on the CCD spectrometer. Fig. 4(B) shows on a magnified scale the emission characteristics of all six dye-sensitised titania films. In every case, the emission was strongly suppressed and indeed only the Fluorescein sensitised film had an emission spectrum that was (barely) detectable above the baseline. Hence, it is evident that depositing a diffuse monolayer of dye molecules on a nanoporous titania scaffold is a highly effective method of suppressing emission, and provides a simple means of fabricating colour filters with negligible autofluorescence.

To further evaluate the dye-sensitised titania filters, we applied them to the fluorescence detection of Rhodamine 6G (R6G), using a 442 nm HeCd laser for optical excitation. Four-layer FDS- and Alizarin-sensitized titania stacks were selected as long-pass filters, both of which were chosen for their ability to provide good blocking of the excitation signal, whilst allowing a significant fraction of the emission signal to pass. To mimic the situation in a typical microfluidic device, the detection configuration shown in ESI Fig. 2† was used, in which the laser spot and Si

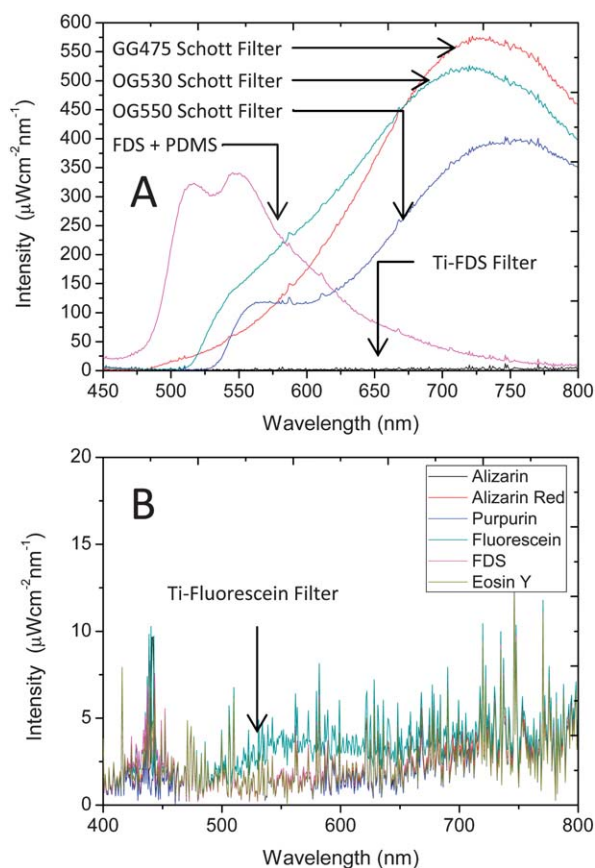


Fig. 4 (A) Autofluorescence spectra for the three Schott Glass colour filters, the Fluorescein salt doped PDMS and the Fluorescein salt sensitised titania filter. All samples were excited at 442 nm with an integration time of 15 min. (B) Autofluorescence spectra for the six dye-sensitised titania films under the same conditions. Note, the spectra are shown on a magnified scale relative to 4(A).

photodiode were positioned opposite one another on the front and back surfaces of a 0.5 mm cuvette, with the long-pass filter tightly inserted between the rear of the cuvette and the photodiode. For comparative purposes, the measurements were repeated using the Schott glass colour filter OG530.

Identical 0.5 mm path-length cuvettes containing different concentrations of R6G in ethanol were prepared in the concentration range 5×10^{-6} to 10^{-3} M. Each cuvette was in turn placed in front of the filter as shown in ESI Fig. 2,† and the intensity on the photodetector was recorded for each one. Fig. 5 shows the signal *versus* R6G concentration for measurements obtained using the four-layer FDS-sensitised titania stack, the four-layer Alizarin-sensitised titania stack, and the commercial Schott glass filter OG530, correcting in all cases for the background current of 0.1 nA. Good linearity was observed from the titania-based filters, with relatively low *y*-axis intercepts of 57.4 nA for Ti-FDS and 11.2 nA for Ti-Alizarin, attributable to incompletely absorbed laser light. Defining the limit of detection Λ as the concentration of analyte that yields a signal equal to the *y*-intercept plus three times the standard deviation of the blank, we obtained $\Lambda = 2.5 \times 10^{-6}$ M ($1.2 \mu\text{g ml}^{-1}$) for the FDS-sensitised filter, and $\Lambda = 1.9 \times 10^{-6}$ M ($0.91 \mu\text{g ml}^{-1}$) for the Alizarin-

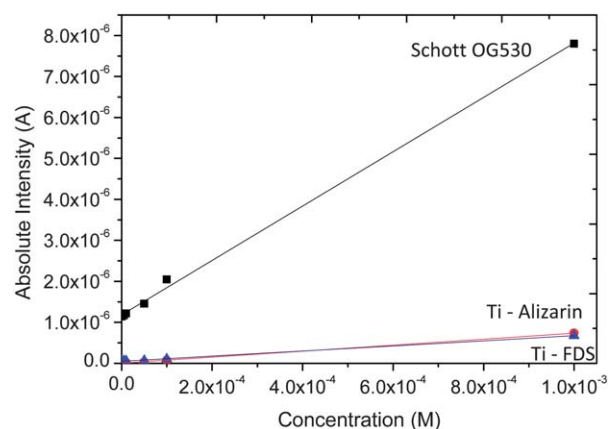


Fig. 5 Signal *versus* concentration of Rhodamine 6G in ethanol using four-layer FDS- and Alizarin-sensitised titania stacks and the Schott glass colour filter OG530 (for long pass filtering). In each case, the light source was a 110 mW HeCd Laser attenuated with O.D. 2 neutral density filter. The light was detected using an amplified Si photodiode and a Keithley 6517 electrometer.

sensitised filter. A much higher *y*-axis intercept of 1.14 μA was observed with the OG530 Schott filter due to strong autofluorescence from the filter, resulting in a significantly worsened limit of detection of $\Lambda = 9.3 \times 10^{-6}$ M ($4.43 \mu\text{g ml}^{-1}$). Hence, in this case it is autofluorescence from the filter that determines the limit of detection of the measurement.

It is apparent from the data in Fig. 3 and 4 that coating nanocrystalline titania with a monolayer of suitably chosen dye molecules offers an effective means of creating colour filters with good blocking characteristics and negligible autofluorescence. However, since titania is widely used as a photocatalyst, it is pertinent to ask whether such filters can be stable under sustained illumination? With this in mind, single-layer FDS- and Alizarin-sensitised filters were loaded into a fluorimeter (Fluoromax-2, Horiba Jobin Yvon) and exposed to 442 nm monochromatic light at a power density of 0.04 mW cm^{-2} . Fig. 6A and B show transmission spectra of the FDS- and Alizarin-sensitised titania

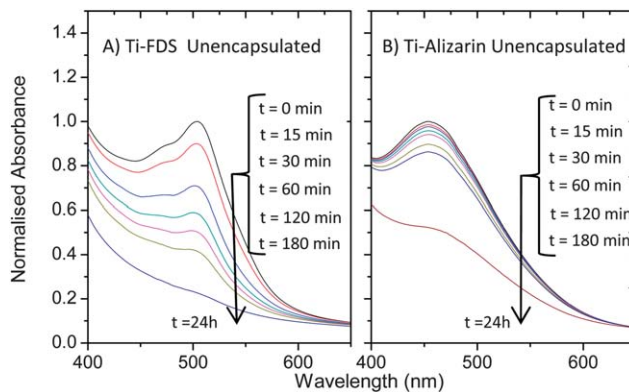


Fig. 6 Evolution of the absorption spectra of unencapsulated single-layer titania films sensitised with (A) FDS and (B) Alizarin under continuous exposure to 0.04 mW cm^{-2} , 442 nm monochromatic light in air.

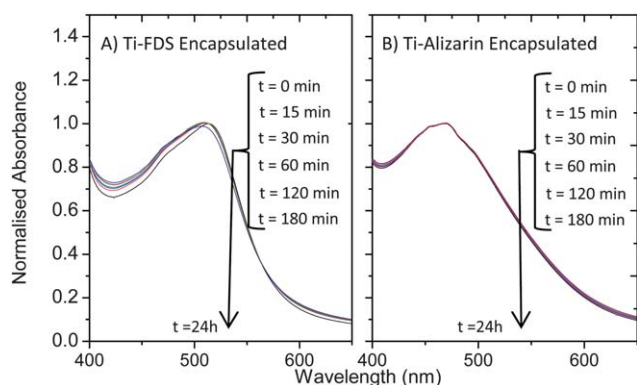


Fig. 7 Evolution of the absorption spectra of glass-encapsulated single-layer titania films sensitised with (A) FDS and (B) Alizarin under continuous exposure to 0.04 mW cm^{-2} , 442 nm monochromatic light in air.

filters after 0, 5, 15, 30, 60, 120, 180 min and 24 h of continuous illumination in air. For both dye-systems progressive degradation of the transmission characteristics is evident over the course of a few hours, significantly limiting their viability as practical filters (note, this is not unexpected, the selected dye molecules are known to be susceptible to photodegradation^{30,31}).

To minimise water- and oxygen-mediated degradation, *fresh* FDS- and Alizarin-sensitised single-layer filters were placed in a dry N_2 environment, briefly annealed to drive off water, and then sealed with a glass cover slide using a UV-curable liquid epoxy (EE-1 Encapsulation Epoxy, Ossila) to provide full glass-encapsulation.

Fig. 7A and B show absorption spectra for the encapsulated filters obtained in air over the course of 24 h (using the same fluorometer settings as before); it is evident from the minimally changing nature of the spectra that encapsulation provides a very effective means of slowing the rate of photo-degradation. The stability of the encapsulated filters is easily sufficient for low cost diagnostic applications where devices are of a use-once disposable nature, and is likely also to be adequate for many repeat-usage applications where stability demands are greater. Further stability improvements can be expected through the use of *colour-fast* dye molecules and/or more stringent encapsulation procedures.

Conclusions

In conclusion, we report a new type of colour filter with minimal autofluorescence that offers a viable low cost alternative to interference filters. The colour filters are prepared by overnight immersion of a substrate coated with highly porous nanoscale titania in an appropriate dye solution, followed by repeated washing to remove excess dye, resulting in monolayer coverage of the dye molecules on the diffuse titania surface. The interface between the titania and the dye molecule induces efficient quenching of photogenerated excitons in the dye molecule, reducing the photoluminescence quantum yield to a negligible value. The approach can be applied to a wide variety of dye molecules, providing they bind strongly to the titania surface and have compatible energy levels to ensure efficient electron transfer

to the titania (note, in circumstances where the dye does not bind directly to the titania surface, a linker unit can be used to anchor the dye³²). The resultant filters exhibit far lower autofluorescence than equivalent filters obtained by dispersing the same molecules in a host matrix, *i.e.* conventional colour filters, and are shown here to outperform such filters in bio-analytical applications, yielding significantly improved limits of detection.

Finally we note that—although the titania films used here were sintered at 450°C , restricting their use to glass and other thermally resilient substrates—they should also be compatible with fabrication on plastic substrates, using *e.g.* a combination of microwave-induced sintering³³ and thin-film encapsulants. This is the subject of continuing work.

Acknowledgements

The research leading to these results has received funding from the European Community's Seventh Framework Programme (FP7/2007–2013) under grant agreement N°248052 (PHOTO-FET). We also acknowledge financial support from the Korea Industrial Technology Foundation (KOTEF).

References

- 1 G. M. Whitesides, *Nature*, 2006, **442**, 368.
- 2 O. Hofmann, P. Miller, P. Sullivan, T. S. Jones, J. C. deMello, D. D. C. Bradley and A. J. deMello, *Sens. Actuators, B*, 2005, **106**, 878.
- 3 B. Yao, G. Luo, L. Wang, Y. Gao, G. Lei, K. Ren, L. Chen, Y. Wang, Y. Hu and Y. Qiu, *Lab Chip*, 2005, **5**, 1041–1047.
- 4 O. Hofmann, X. Wang, J. C. deMello, D. D. C. Bradley and A. J. deMello, *Lab Chip*, 2005, **5**, 863.
- 5 X. Wang, O. Hofmann, R. Das, E. M. Barrett, A. J. deMello, J. C. deMello and D. D. C. Bradley, *Lab Chip*, 2007, **7**, 58.
- 6 J. B. Edel, N. P. Beard, O. Hofmann, J. C. deMello, D. D. C. Bradley and A. J. deMello, *Lab Chip*, 2004, **4**, 136.
- 7 D. Brennan, J. Justice, B. Corbett, T. McCarthy and P. Galvin, *Anal. Bioanal. Chem.*, 2009, **395**, 621.
- 8 Q. Kou, I. Yesilyurt, V. Studer, M. Belotti, E. Cambril and Y. Chen, *Microelectron. Eng.*, 2004, **73–74**, 876.
- 9 S. Moon, H. O. Keles, A. Ozcan, A. Khademhosseini, E. Hægström, D. Kuritzkes and U. Demirci, *Biosens. Bioelectron.*, 2009, **24**, 3208–3214.
- 10 E. Thrush, O. Levi, L. J. Cook, J. Deich, A. Kurtz, S. J. Smith, W. E. Moerner, J. James and S. Harris, *Sens. Actuators, B*, 2005, **105**, 393.
- 11 N. Chronis, G. L. Liu, K. H. Jeong and L. P. Lee, *Opt. Express*, 2003, **11**, 2370.
- 12 O. Hofmann, X. Wang, A. Cornwell, S. Beecher, A.-B. Raja, D. D. C. Bradley, A. J. deMello and J. C. deMello, *Lab Chip*, 2006, **6**, 981.
- 13 S. Kostner and M. J. Vellekoop, *Part. Part. Syst. Charact.*, 2008, **25**, 92.
- 14 K. Hosokawa, K. Hanada and R. Maeda, *J. Micromech. Microeng.*, 2002, **12**, 1.
- 15 S. Balslev, A. M. Jorgensen, B. Bilenberg, K. B. Mogensén, D. Snakenborg, O. Geschke, J. P. Kutter and A. Kristensen, *Lab Chip*, 2006, **6**, 213.
- 16 R. Irawan, S. C. Tjin, X. Fang and C. Y. Fu, *Biomed. Microdevices*, 2007, **9**, 413.
- 17 A. Banerjee, A. Pais, I. Papautsky and D. Klotzkin, *IEEE Sens. J.*, 2008, **8**, 621.
- 18 L. Andreu, Stefanie Demming, Haakan N. Joensson, J. Vila-Planas, H. Andersson-Svahn and S. Büttgenbach, *Lab Chip*, 2010, **10**, 1987.
- 19 C. Bliss, J. N. McMullin and C. J. Backhouse, *Lab Chip*, 2008, **8**, 143.
- 20 G. Minas, R. F. Wolffenbuttel and J. H. Correia, *Lab Chip*, 2005, **5**, 1303.

- 21 C. Richard, A. Renaudin, V. Aimez and P. G. Charette, *Lab Chip*, 2009, **9**, 1371.
- 22 M. Gratzel, *J. Photochem. Photobiol., A*, 2004, **164**, 3.
- 23 R. Huber, S. Spörlein, J. E. Moser, M. Grätzel and J. Wachtveitl, *J. Phys. Chem. B*, 2000, **104**, 8995–9003.
- 24 T. Hannappel, B. Burfeindt and W. Störck, *J. Phys. Chem. B*, 1997, **101**, 6799.
- 25 P. V. Kamat, *Prog. React. Kinet.*, 1994, **19**, 277.
- 26 J. E. Moser and M. Grätzel, *Chem. Phys.*, 1993, **176**, 493.
- 27 Y. Tachibana, J. E. Moser, M. Grätzel, David R. Klug and J. R. Durrant, *J. Phys. Chem.*, 1996, **100**, 20056.
- 28 C. Miliani, A. Romani and G. Favaro, *Spectrochim. Acta, Part A*, 1998, **54**, 581–588.
- 29 P. Meallier, S. Guittonneau, C. Emmelin and T. Konstantinova, *Dyes Pigm.*, 1999, **40**, 95–98.
- 30 L. Song, E. J. Hinnick, I. Ted Young and H. J. Tanke, *Biophys. J.*, 1995, **68**, 2588.
- 31 C. Chen and C. Chen, *J. Phys. Chem. B*, 2002, **106**, 318.
- 32 N. Koumura, Z.-S. Wang, S. Mori, M. Miyashita, E. Suzuki and K. Hara, *J. Am. Chem. Soc.*, 2006, **128**, 14256.
- 33 S. Uchida, M. Tomiha, H. Takizawa and M. Kawanaya, *J. Photochem. Photobiol., A*, 2004, **164**, 93.